

# Notes

## Mechanical Properties of Cross-Linked Hyaluronic Acid/Poly-(L-lysine) Multilayer Films

Dominique Collin,<sup>†</sup> Philippe Lavalley,<sup>\*,‡</sup>  
Juan Méndez Garza,<sup>‡,§</sup> Jean-Claude Voegel,<sup>‡</sup>  
Pierre Schaaf,<sup>‡</sup> and Philippe Martinoty<sup>†</sup>

Laboratoire de Dynamique des Fluides Complexes (CNRS/ULP UMR 7506), Université Louis Pasteur, 4 rue Blaise Pascal, 67070 Strasbourg Cedex, France; INSERM Unité 595, Faculté de Chirurgie Dentaire, Université Louis Pasteur, 11 rue Humann, F-67085 Strasbourg Cedex, France; Mécanique et Ingénierie Cellulaire et Tissulaire, UMR CNRS 7563-LEMTA, Faculté de Médecine, 54500 Vandœuvre-lès-Nancy, France; and Institut Charles Sadron (CNRS UPR 22), 6 rue Boussingault, F-67083 Strasbourg Cedex, France

Received June 30, 2004

Revised Manuscript Received September 15, 2004

The sequential assembly of polyanions and polycations onto a solid substrate leads to the formation of films that regularly grow and are called “polyelectrolyte multilayers”. Introduced in 1991 by Decher and Hong,<sup>1,2</sup> these films have received considerable attention since then due to potential applications in fields as different as electroluminescent devices, separation processes,<sup>3</sup> or biomaterial coatings.<sup>4</sup> Two types of films were realized: linearly growing films<sup>2</sup> and exponentially growing ones.<sup>5,6</sup> The linear growing films consist of stacked polyelectrolyte layers, which interpenetrate each other, leading to a periodic structure in a direction perpendicular to the layers.<sup>7</sup> The typical thickness of a polyanion/polycation bilayer can vary from 1 nm up to several tens of nanometers depending on the pH and salt concentration of the solution used during film buildup.<sup>8</sup> Poly(styrenesulfonate)/polyallylamine,<sup>2</sup> poly(acrylic acid)/polyallylamine,<sup>8</sup> or poly(styrenesulfonate)/poly(diallyldimethylammonium)<sup>9</sup> constitute a few prominent examples of such types of films. Exponentially growing films were essentially obtained with systems composed of natural polyelectrolytes and poly(amino acid)s. These films are much less structured and are highly hydrated. Hyaluronic acid/polylysine,<sup>5</sup> poly(glutamic acid)/polylysine,<sup>10</sup> and poly(glutamic acid)/polyallylamine<sup>11</sup> constitute some of the well-characterized examples of this type of film which could be well appropriated for biomaterial coatings.

All these linearly or exponentially growing films were extensively characterized in terms of physicochemical parameters: in particular thickness, roughness,

porosity, charge density of the outer layer, internal structure, etc. On the other hand, much less attention was paid on dynamical parameters such as the polyelectrolyte diffusion coefficients within these films, even if some data exist,<sup>5</sup> or on the mechanical properties of the film itself. The knowledge of the mechanical properties of polyelectrolyte multilayer films is of primary importance for their applications, like the buildup of self-supporting membranes. Also, these properties seem to play a role in the interactions between cells and surfaces, cellular adhesion being favored on “hard” materials.<sup>12</sup> For example, it is known that chondrosarcoma cells adhere only weakly on poly(L-lysine)/hyaluronic acid (PLL/HA) multilayer films and much strongly when these polyelectrolyte multilayers are chemically cross-linked.<sup>13</sup> The relatively small number of data available for the mechanical parameters of polyelectrolyte multilayers can be associated with the experimental difficulty of their measurements. Three methods of measurements were reported: (i) determination of elastic modulus and tensile strength on self-supporting polyelectrolyte membranes, which always contained nanoparticles or nanotubes in order to greatly enhance their ultimate tensile stress;<sup>14,15</sup> (ii) elasticity measurements from indentation curves of an AFM tip or a colloidal particle deposited on the cantilever tip;<sup>16</sup> (iii) determination of the elastic properties of polyelectrolyte capsules. The Young’s moduli measured in all these experiments are summarized in Table 1.

In this note we present new data for the PLL/HA multilayer films obtained by using a piezo-rheometer. This new type of rheometer allows the first determination of the complex shear modulus over a wide frequency range, from 0.2 Hz to a few kilohertz. This technique requires films with thicknesses ranging from 10 to 100  $\mu\text{m}$  and is thus well adapted for the study of thick exponentially growing films.

The (PLL/HA)<sub>n</sub> multilayer films were built up by sequential dipping of the substrate into polyanion and polycation solutions. Once formed, they were cross-linked using 1-ethyl-3-(3-(dimethylamino)propyl)carbodiimide in the presence of *N*-hydroxysulfosuccinimide (see Supporting Information). Confocal microscopy and the piezo-rheometer were used to visualize the films and to measure their mechanical properties, respectively. In the case of the mechanical measurements, the substrate was a thick glass slide (called thereafter the sample-bearing glass slide), which will be stuck to the emitting glass slide of the piezo-rheometer cell (see Figure 1). The piezo-rheometer allows the determination of the complex shear modulus  $G = G' + iG''$ .<sup>22–27</sup> The principle of this apparatus is shown in Figure 1. It consists of applying a small strain to the sample by means of two identical piezoelectric ceramics vibrating in the shear mode and measuring the amplitude and the phase  $\varphi$  of the shear stress transmitted through the sample using a second receiving piezoelectric ceramic. The complex

<sup>†</sup> CNRS/ULP UMR 7506, Université Louis Pasteur.

<sup>‡</sup> INSERM Unité 595, Université Louis Pasteur.

<sup>§</sup> UMR CNRS 7563-LEMTA.

<sup>‡</sup> Institut Charles Sadron.

\* Corresponding author: Tel 00 33 3 90 24 30 61; Fax 00 33 3 90 24 33 79; e-mail philippe.lavalley@odonto-ulp.u-strasbg.fr.

**Table 1. Young's Moduli of Multilayer Films with Various Compositions**

multilayer composition (growth regime)	no. of pair of layers deposited	Young's moduli	method	ref
poly(styrenesulfonate)/poly(allylamine hydrochloride) PSS/PAH (linear)	10	1.5–2.1 GPa	osmotic pressure on capsules	17
PSS/PAH (linear)	10	1.3–1.9 GPa	capsule deformation by AFM	18
PSS/PAH (linear)	4	100–200 MPa	capsule deformation by AFM	19
PSS/PAH with a gold nanoparticle layer (linear)	7/gold/7	30–40 GPa	self-supporting membrane	15
polyethylenimine/carbon nanotubes (linear)	5	220 GPa <sup>a</sup>	self-supporting membrane	14
PAH/polyazobenzene (linear)	346 at pH 5.0 560 at pH 7.0 116 at pH 9.0 76 at pH 10.5	6 MPa 1.5 MPa 100 kPa 100 kPa	AFM nanoindentation	16
poly(allylamine hydrochloride)/poly(acrylic acid) (linear)	8, 45, 600	70 MPa	nanoindenter	20
poly(L-lysine)/hyaluronic acid PLL/HA (exponential)	20, 40, 60	40–90 kPa	AFM nano-indentation of colloidal probe	21

<sup>a</sup> Ultimate tensile strength.

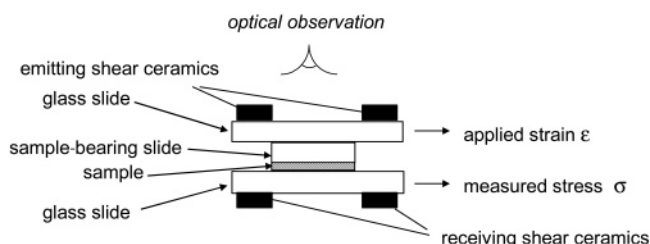


**Figure 1.** Schematic representation of the piezo-rheometer cell.

shear modulus of the sample is given by the stress over strain ratio  $G = \sigma/\epsilon$ . The material has an elastic response when the strain and the stress are in-phase ( $\varphi = 0$ ) and a viscous response when the strain and the stress have a phase difference  $\varphi$  of  $90^\circ$ . For a viscoelastic material, the phase difference  $\varphi$  lies between  $0^\circ$  and  $90^\circ$ . All the experimental details are given in the Supporting Information.

Our experiments were performed on multilayer films made of 90 (PLL/HA) bilayers. These films were very homogeneous in the bulk, with top and bottom surfaces which were flat, as shown by Figure 2 obtained by confocal laser scanning microscopy (CLSM) (see also Figure 1 in the Supporting Information).

The thickness of the film measured by CLSM was around  $32\ \mu\text{m}$ . The film appeared greener on top of the film compared to its bottom. This is generally observed for exponentially growing films when the thickness exceeds several tens of micrometers. It may be due to the fact that adsorption of PLL<sup>FITC</sup> (see Supporting Information) for 10 min followed by a 10 min rinse before cross-linking is too short to allow a complete diffusion and exchange process over the whole film thickness between PLL<sup>FITC</sup> and nonlabeled PLL.<sup>28</sup>

Some outgrowths sometimes appeared on the edges of the film when the sample-bearing glass slide was separated from its holder and stuck on the emitting glass slide of the piezo-rheometer cell (see Figure 1). Then, this sample-bearing glass was stuck on one of the glass slide of the piezo-rheometer cell (see Figure 2). These outgrowths are disturbing because they modify the value of the shear modulus. Great care was therefore taken to minimize their formation.

Figure 3 gives typical results obtained at room temperature and showing the behavior of  $G'$  measured at 1 Hz as a function of the gap  $L$  between the sample-bearing glass slide and the receiving glass slide of the

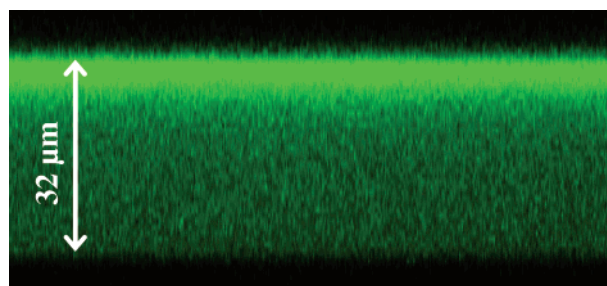


**Figure 2.** Vertical section image of a (PLL/HA)<sub>90</sub>/PLL<sup>FITC</sup> multilayer film in solution (NaCl 0.15 M, pH = 5.9), observed by CLSM. Film thickness is about  $32\ \mu\text{m}$ .

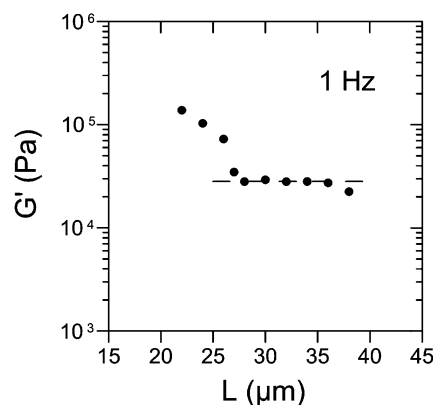


**Figure 3.** Real part  $G'$  of the shear modulus of a (PLL/HA)<sub>90</sub> multilayer film measured at 1 Hz, as a function of the gap  $L$  between the sample-bearing glass slide and the receiving glass slide of the cell.

cell for a (PLL/HA)<sub>90</sub> multilayer film. It can be seen that  $G'$  is zero when  $L$  is higher than  $\sim 38\ \mu\text{m}$ , which is expected since the sample thickness is smaller than  $L$ . A value different from zero appears at  $L \sim 38\ \mu\text{m}$ , i.e., for a gap slightly higher than that measured by confocal microscopy, which suggests the presence of small outgrowths on the edges of the sample. If the sample is compressed,  $G'$  first increases slightly and then remains constant down to a thickness of  $\sim 26\ \mu\text{m}$ , with a value equal to 28 kPa. The fact that  $G'$  does not vary when the thickness of the film decreases from  $\sim 36\ \mu\text{m}$  down to  $\sim 26\ \mu\text{m}$  shows that the shear mechanical properties of the sample are independent of the compression applied to it. This can be explained by the fact that the film is soft and that a compression up to 30% does not strongly modify its structure. This is in agreement with

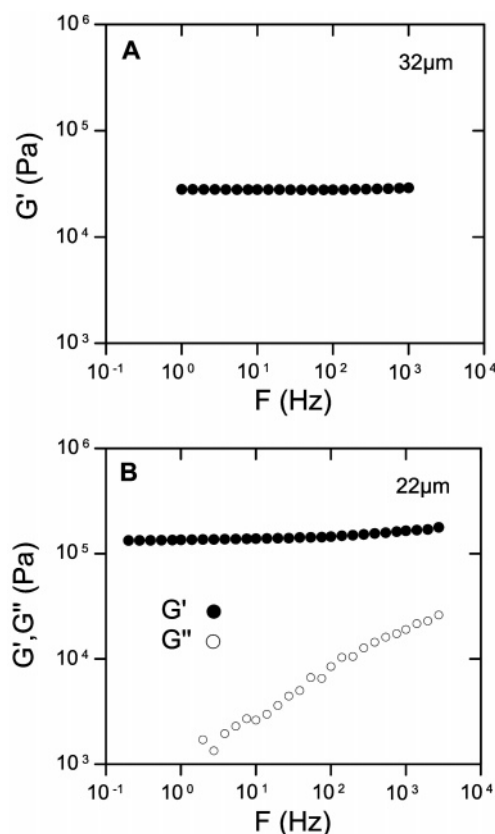


**Figure 4.** (A) Real part  $G'$  of the shear modulus of a (PLL/HA)<sub>90</sub> multilayer film, as a function of the frequency  $F$  for a gap  $L = 32 \mu\text{m}$  between the sample-bearing glass slide and the receiving glass slide of the cell. (B) Real part  $G'$  and imaginary part  $G''$  of the shear modulus of a (PLL/HA)<sub>90</sub> multilayer film, as a function of the frequency  $F$  for a gap  $L = 22 \mu\text{m}$  between the sample-bearing glass slide and the receiving glass slide of the cell.

the picture of exponentially growing films which are highly hydrated and made of layers of polyelectrolyte complexes which can easily interpenetrate each other.<sup>29</sup> The situation dramatically changes when the compression becomes stronger, as illustrated by the significant increase of  $G'$  in Figure 3 when the thickness becomes smaller than  $L \sim 26 \mu\text{m}$ . This change in behavior could be due to an increase of the polyelectrolyte interactions induced by the compression of the film. Note that macroscopic cracks are observed in the sample when the compression becomes too strong, for example, when the thickness of the sample is smaller than  $22 \mu\text{m}$ .

The samples with marked outgrowths at their edges do not show the slight increase of  $G'$  around  $L \sim 38 \mu\text{m}$ , but rather a progressive increase which reflects the contribution of the outgrowths to  $G'$ . The effect of the overcompression of the sample for thicknesses smaller than  $L \sim 26 \mu\text{m}$  is also different since the compression applied is not the same for the outgrowths and the rest of the sample. Consequently, the width of the plateau is reduced, but its value remains of the order of 28 kPa and therefore represents the intrinsic value of the shear modulus of the film.

The behavior of  $G'$  as a function of the frequency for  $L \sim 32 \mu\text{m}$  is shown in Figure 4A. It can be seen that  $G'$  remains constant in the frequency range studied. This result indicates that this film has a pure elastic response in the low-frequency limit and that the characteristic frequency of the slowest relaxation mode is higher than  $10^3$  Hz. This is confirmed by the value of

the phase angle which is zero for all the frequencies studied. The behavior of  $G''$  is not shown in the figure because the  $G''$  values are too small to be determined. The frequency response of the samples with  $L$  ranging from  $\sim 26$  to  $38 \mu\text{m}$  is the same as that for  $L \sim 32 \mu\text{m}$  sample. This response dramatically changes when the sample is overcompressed, as shown by Figure 4B obtained for  $L \sim 22 \mu\text{m}$ . It can be seen that  $G'$  is no more constant over the whole frequency range studied and starts to increase for frequencies higher than  $10^2$  Hz. This overcompression also induces an increase of  $G''$  and of the associated viscosity (the sliding is less easy), which can be measured now. These  $G'$  and  $G''$  behaviors indicate that the overcompression strongly reduces the characteristic frequency of the slowest relaxation mode of the system.

If we assume that the film behaves as an isotropic medium, the shear modulus  $G$  of the film is related to its Young's modulus  $E$  by the relationship  $E = 3G$ . An estimate of  $E$  can therefore be given, and  $E$  is found to be of the order of 84 kPa. As expected, this value is much smaller than the Young's moduli measured on linearly growing films and reported in Table 1. On the other hand, the Young's modulus we measure is of the same order of magnitude as that measured by Richert et al.<sup>21</sup> on similar exponentially growing films, using AFM nanoindentation of colloidal probe. Hyaluronic acid present in the PLL/HA films is probably also responsible for this relative low value of Young's modulus. This is confirmed by previous study on soft gels of hyaluronic acid describing Young's moduli between 3 and 250 Pa.<sup>30</sup>

A piezorheometer has been used to provide the first study of the shear modulus of multilayer polyelectrolyte films. The results show that these films present a purely elastic response in the frequency range  $1\text{--}10^3$  Hz. This response is not modified when the films are submitted to a static compression as high as  $\sim 30\%$ , which is consistent with the picture of hydrated films with layers interpenetrating each other. These systems, which behave like a chemical gel in the hydrodynamic limit, are characterized by a shear modulus on the order of 30 kPa corresponding to a Young's modulus of the order of 90 kPa, much smaller than all the known elastic moduli measured for linearly growing films. These results demonstrate the interest of the piezo-rheology technique for the elastic properties determination of soft and brittle materials.

**Acknowledgment.** J.M.G. is indebted to CONACyT (Consejo Nacional de Ciencia y Tecnología, México) and to Prof. J. F Stoltz (UMR CNRS 7563-LEMTA, Nancy) for financial support. We are grateful to Jérôme Mutterer of the Institut de Biologie Moléculaire des Plantes, CNRS/ULP (Strasbourg, France), for his assistance with the CLSM. The CLSM platform used in this study was cofinanced by the Région Alsace, the Université Louis Pasteur, and the Association pour la Recherche sur le Cancer. We also thank Karim Benmlih for his technical assistance.

**Supporting Information Available:** Experimental details and confocal microscopy top view of (PLL/HA)<sub>90</sub>/PLL<sup>FITC</sup> multilayer film (Figure 1). This material is available free of charge via the Internet at <http://pubs.acs.org>.

## References and Notes

- (1) Decher, G.; Hong, J. D. *Makromol. Chem., Macromol. Symp.* **1991**, *46*, 321–327.

- (2) Decher, G. *Science* **1997**, *277*, 1232–1237.
- (3) Liu, X. Y.; Bruening, M. L. *Chem. Mater.* **2004**, *16*, 351–357.
- (4) Thierry, B.; Winnik, F. M.; Merhi, Y.; Silver, J.; Tabrizian, M. *Biomacromolecules* **2003**, *4*, 1564–1571.
- (5) Picart, C.; Lavalle, P.; Hubert, P.; Cuisinier, F. J. G.; Decher, G.; Schaaf, P.; Voegel, J. C. *Langmuir* **2001**, *17*, 7414–7424.
- (6) Elbert, D. L.; Herbert, C. B.; Hubbell, J. A. *Langmuir* **1999**, *15*, 5355–5362.
- (7) Lösche, M.; Schmitt, J.; Decher, G.; Bouwman, W. G.; Kjaer, K. *Macromolecules* **1998**, *31*, 8893–8906.
- (8) Shiratori, S. S.; Rubner, M. F. *Macromolecules* **2000**, *33*, 4213–4219.
- (9) Schlenoff, J. B.; Dubas, S. T. *Macromolecules* **2001**, *34*, 592–598.
- (10) Lavalle, P.; Gergely, C.; Cuisinier, F. J. G.; Decher, G.; Schaaf, P.; Voegel, J. C.; Picart, C. *Macromolecules* **2002**, *35*, 4458–4465.
- (11) Boulmedais, F.; Ball, V.; Schwinte, P.; Frisch, B.; Schaaf, P.; Voegel, J. C. *Langmuir* **2003**, *19*, 440–445.
- (12) Pelham, R. J.; Wang, Y. L. *Proc. Natl. Acad. Sci. U.S.A.* **1997**, *94*, 13661–13665.
- (13) Richert, L.; Boulmedais, F.; Lavalle, P.; Mutterer, J.; Ferreux, E.; Decher, G.; Schaaf, P.; Voegel, J.-C.; Picart, C. *Biomacromolecules* **2004**, *5*, 284–294.
- (14) Mamedov, A. A.; Kotov, N. A.; Prato, M.; Guldi, D. M.; Wicksted, J. P.; Hirsch, A. *Nat. Mater.* **2002**, *1*, 190–194.
- (15) Jiang, C. Y.; Markutsya, S.; Tsukruk, V. V. *Adv. Mater.* **2004**, *16*, 157–161.
- (16) Mermut, O.; Lefebvre, J.; Gray, D. G.; Barrett, C. J. *Macromolecules* **2003**, *36*, 8819–8824.
- (17) Gao, C.; Donath, E.; Moya, S.; Dudnik, V.; Möhwald, H. *Eur. Phys. J. E* **2001**, *5*, 21–27.
- (18) Dubreuil, F.; Elsner, N.; Fery, A. *Eur. Phys. J. E* **2003**, *12*, 215–221.
- (19) Lulevich, V. V.; Andrienko, D.; Vinogradova, O. I. *J. Chem. Phys.* **2004**, *120*, 3822–3826.
- (20) Pavor, P. V.; Bellare, A.; Strom, A.; Yang, D.; Cohen, R. E. *Macromolecules* **2004**, *37*, 4865–4871.
- (21) Richert, L.; Engler, A. J.; Discher, D. E.; Picart, C. *Biomacromolecules* **2004**, *5*, 1908–1916.
- (22) Weilepp, J.; Stein, P.; Assfalg, N.; Finkelmann, H.; Martinoty, P.; Brand, H. R. *Europhys. Lett.* **1999**, *47*, 508–514.
- (23) Weilepp, J.; Zanna, J. J.; Assfalg, N.; Stein, P.; Hilliou, L.; Mauzac, M.; Finkelmann, H.; Brand, H. R.; Martinoty, P. *Macromolecules* **1999**, *32*, 4566–4574.
- (24) Stein, P.; Assfalg, N.; Finkelmann, H.; Martinoty, P. *Eur. Phys. J. E* **2001**, *4*, 255–262.
- (25) Zanna, J. J.; Stein, P.; Marty, J. D.; Mauzac, M.; Martinoty, P. *Macromolecules* **2002**, *35*, 5459–5465.
- (26) Martinoty, P.; Hilliou, L.; Mauzac, M.; Benguigui, L.; Collin, D. *Macromolecules* **1999**, *32*, 1746–1752.
- (27) Collin, D.; Martinoty, P. *Physica A* **2003**, *320*, 235–248.
- (28) Lavalle, P.; Vivet, V.; Jessel, N.; Decher, G.; Mesini, P. J.; Voegel, J.-C.; Schaaf, P. *Macromolecules* **2004**, *37*, 1159–1162.
- (29) Picart, C.; Mutterer, J.; Richert, L.; Luo, Y.; Prestwich, G. D.; Schaaf, P.; Voegel, J. C.; Lavalle, P. *Proc. Natl. Acad. Sci. U.S.A.* **2002**, *99*, 12531–12535.
- (30) Ladam, G.; Vonna, L.; Sackmann, E. *J. Phys. Chem. B* **2003**, *107*, 8965–8971.

MA048683G